SMiRT-12 / K. Kussmaul (Editor)

C07/3

ANALYSIS OF THE INTERACTION BETWEEN FUEL ELEMENTS AND SUPPORTING GRID IN LOCA CONDITIONS

C.A. de Oliveira[1] and R. de Noronha[2]

[1]IPEN/COPESP, Travessa R, 400, Cid. Universit., 05508 São Paulo, SP - Brasil
[2]COPESP, av. Lineu Prestes 2242, 05508 São Paulo, SP - Brasil

ABSTRACT

The dynamic interaction caused by LOCA loads between two internal structures of PWR type nuclear reactors, the fuel elements and the supporting grid, was analyzed with finite elements. The fuel elements are considered to be laid on the grid and compressed against it by means of springs located on the top of the elements. The results of the analysis showed that impacts occur between the components. The forces and stresses caused by the fuel elements on the grid were evaluated.

INTRODUCTION

For nuclear plants licensing, the verification that the system preserves its shutdown capability when submitted to a LOCA, Loss Of Coolant Accident, is a basic requirement in reactor safety [1,2]. The case usually considered to be most severe and emphasized in pressure vessel assessments is a double-ended break of a main coolant loop pipe, usually assumed to occur between the vessel inlet nozzle and the pump [3]. This event produces a decompression wave that propagates through the piping and equipment [1,4].

The design requirement is that the primary system must withstand the forces caused by the postulated break without additional ruptures which would either reduce core cooling or exceed the containment pressure design value. For the reactor, this requirement is considered to be met when its internal structures satisfy the limits of the Appendix F of Section III of the ASME Code, "Rules for Evaluation of Service Loadings with Level D Service Limits" [5].

The present work analyses the interaction between two internal components of PWR type nuclear reactors, the fuel elements and the supporting grid, in the event of a cold leg LOCA. Attached to the grid, there is a flow distribution plate. In this way, with the LOCA, the pressure gradients caused by the decompression wave propagation would produce vibrations on the plate-grid set. The fuel elements are only laid on the grid and compressed against it by means of springs located on the top of the elements. The vibrations of the grid could produce the separation of the fuel elements from the grid, and subsequent impacts when they contact back again.

FINITE ELEMENT MODEL

LOCA analyses are more accurate with coupled fluid-struture models. However, these models are considerably more difficult to solve than the isolated uncoupled models, primarily because of the difficulty of dealing with the combined size of a fluid and structural model [6]. On the other hand, uncoupled procedures may be very conservative because the rigid wall loads will always be greater than the loads on the actual flexible structure [6,7].

Taking into account the economical advantages, an uncoupled model was preferred for this analysis. Fluid-structure interaction should be considered later if the stresses calculated from the uncoupled analysis are found to be too high. Also, three dimensional fluid effects were not considered important in order to model the lower grid region. In this way, the unidimensional finite difference program RELAP4 was employed to model the fluid while the general purpose finite element ANSYS program, version 4.4A [8], was used for the structure. This text is not concerned with the fluid modelling, which is detailed in [9]. The following paragraphs give information on the F. E. model used for the structure.

The finite element model is shown in figure 1. The grid ring was modelled with solid 3D elements while the grid beams and the flow distribution plate were modelled with 3D shells. Taking into account the symmetry of the model and of the loading with respect to the planes OXZ and OYZ, symmetry restrictions were applied on the nodes located on these two planes. Since the grid is connected to the barrel through pins and bolts, the nodes of the ring which approximated the bolt positions were restricted on the vertical Z direction, and the nodes that approximated the pins had their transverse directions X and Y restricted.

Since the grid model contained a large number of degrees of freedom, the substructuring technique was applied to condense the model. For the generation of the super-element, only 20 degrees of freedom were preserved. Eight of them were manually selected and the others were chosen during the condensation process, retaining the degrees of freedom with smallest K/M ratio.

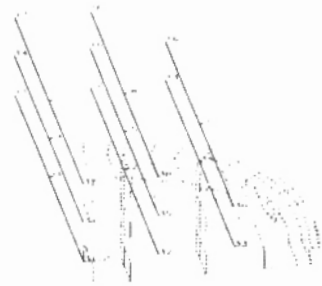

Fig 1: Finite element model.

The substructuring technique is only applicable to the linear portions of finite elements models. Therefore, the non-linear part, consisting of the fuel elements with its upper and lower gaps, was modelled separately and connected to the 8 manually selected master degrees of freedom of the super-element through constraint equations. Each fuel element set consisted of 3 nodes and 4 elements (of mass, truss and gap). The fuel element itself was modelled with a mass element. To model the stiffness and pre-deformation of the fuel element springs, a truss element was employed. Two gaps were modelled, the first, simulating the spacing between the fuel element and the upper core plate, was inserted in parallel to the truss element. The second, without

initial spacing, simulates the contact between the fuel element and the lower grid.

In this way, the fuel elements were modelled as rigid bodies of concentrated mass. In the event of an impact with the grid, the fuel elements will not behave in this manner since the friction with the spring clips will not be sufficient to avoid the sliding of the fuel rods. However, to assume that the fuel elements have rigid body behavior is conservative for the lower grid, the internal that is to be analyzed. As shown in figure 1, eight fuel elements were modelled, jointly with its springs and gaps. The fuel elements of figure 1 were ordered in the following manner: fuel element i: formed by nodes 1i, 2i and 3i, i varying from 1 to 8.

For the sets located at the symmetry planes OXZ and OYZ, fuel elements 2, 3, 4 and 7, the fuel element mass and the values of the truss and gap stiffnesses were reduced by one half, while for the set located at the Z axis, that is, fuel element number 1, the fuel element mass and the truss and gap stiffnesses were reduced to one fourth.

LOADINGS

The pressure transient due to cold leg LOCA and the weight of the structure were considered. In a LOCA analysis, the simultaneous occurrence of a Safe Shutdown Earthquake, SSE, should be assumed. In the present analysis, however, these loads were considered to be negligible. The pressure transient was established by means of the thermo-hidraulic program RELAP4 [9]. A double ended break in the cold leg, near the reactor nozzle, was considered in order to generate the transient. To capture the pressure wave, a time step of 10^{-4}s was used.

Figure number 2 gives the values of pressure above, below and the pressure difference across the grid as a function of integration step (1 step = 10^{-4}s). The maximum of this difference occurs at 3.9ms. As shown in figure 2, this maximum is caused by the relative pressure fluctuation between the volumes above and underneath the grid, during the depressurization phase. Figure 3 clearly shows that the pressure gradient on the grid is completely negligible from 0.035s onwards. This pressure gradient was applied directly on the shell elements modelling the distributor plate.

RESULTS

The non-linear integration was performed with the ANSYS program through the Newmark method. Through an analysis of the characteristics of the gaps, of the excitation frequencies and of the natural frequencies of the structure, an integration time step of $2*10^{-5}$s was found to be necessary. Since the values of the pressure gradient were available only in intervals of 10^{-4}s, a linear interpolation scheme was used to obtain the values within the time intervals. The solution was carried up to only 29.5ms. The results are presented in the following paragraphs.

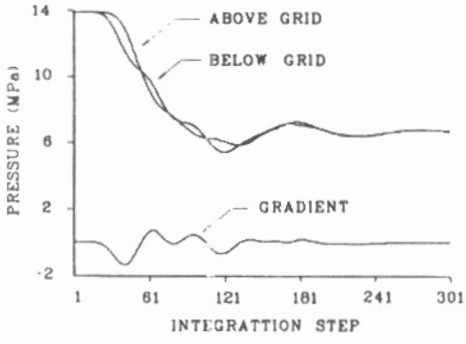

Fig 2: Pressures above and below grid and gradient, from 0 to 0.03s.

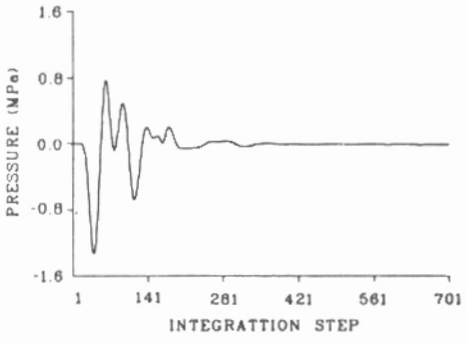

Fig 3: Pressure differences across the grid, from 0 to 0.07s.

The closure forces of the lower gaps are shown in figure 4. These are the impact forces between the fuel bundles and the grid. Impacts of all fuel elements on the grid took place between instants 5.38ms and 5.44ms, agreeing with the first peak of fig 4. Fuel elements 1, 2 and 4 had their maximum impact forces in this point. Fuel elements 3, 5 and 7 had their maximum impact forces between 6.66ms and 6.70ms, agreeing with the second peak of fig 4. Finally, fuel elements 6 and 8 had their maximum impact forces around 0.025s, the third and fourth peaks of figure 4. Closure of the upper gap elements did not occur, that is, the fuel elements did not impact the upper core plate.

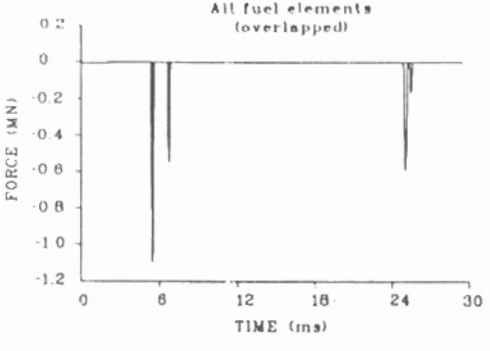

Fig 4: Impacts on the lower gaps.

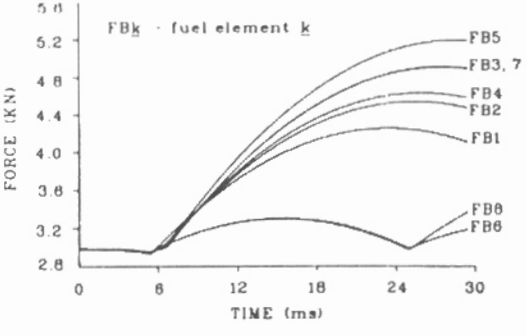

Fig 5: Compression forces on the truss elements.

The compression forces on the truss elements, which represent the forces of the fuel elements springs, are presented in figure 5. Taking into account that the upper nodes of the truss elements have their displacements restricted, the curves of figure 5 represent the "trajectory" of the fuel elements when interacting with the grid. In the beginning, due to the lowering of the grid, all fuel elements fall together. With the rise of the grid, after the passage of the depression peak, impacts occur and the fuel elements are thrown upwards. Fuel elements 6 and 8, being near the grid ring, receive smaller impacts and fall again. Fuel elements 1, 2 and 4, being nearer the grid

center, receive much larger impacts and do not fall back into the grid within the integration time interval. Finally fuel elements 3, 5 and 7, which are in an intermediate position, do not gain sufficient velocity in the first impact, being impacted twice and then receiving enough energy to be thrown over the central fuel elements. The minimum of these forces indicate that the time instant of maximum downward movement of the fuel elements occurs around 5.37ms.

The generalized displacements of the master degrees of freedom connected to the fuel elements are shown in figure 6. These degrees of freedom have their maximum displacements at 4.44ms or 4.46ms. The other vertical degrees of freedom, as well as most of the transverse ones have their displacement peaks also near these two instants. Accordingly, it can be said that the grid suffers a maximum vertical and lateral deformation between 4.42ms and 4.48ms, just after the peak of the pressure transient, which occurs at 3.9ms. In this time interval of maximum grid deformation, all fuel elements are separated from the grid.

The first impact of the fuel elements with the grid occurs almost simultaneously between 5.38 and 5.44ms which, according to figure 6, corresponds to a reversal of the movement of the grid, but not to high deformation. These impact forces will produce high stresses in local regions of the grid. These stresses, however, are characterized as secondary stresses and, as shall be discussed next, are not important in LOCA analyses. Furthermore, the representation of the fuel elements as rigid bodies is extremely conservative for the analysis of the impacts on the grid.

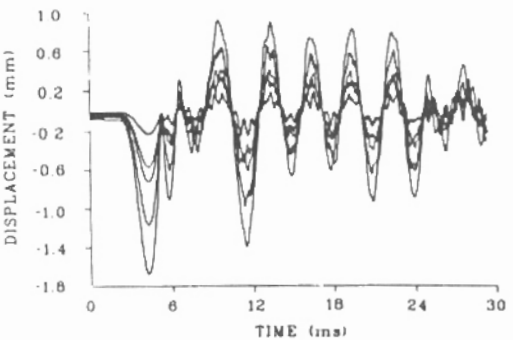

Fig 6: Displacements of the master DoFs connected to the fuel elements.

STRESS VERIFICATIONS

Appendix F of Section III of the ASME Code [5], which is applicable to LOCA analyses, establishes limits only to general membrane (P_m), local membrane (P_L) and membrane plus bending (P_L+P_b) primary stress intensities. For the instants of maximum deformation, from 4.42ms to 4.48ms, the solution was expanded, obtaining in this way the stresses in the grid. The nodal values of stress intensity were calculated separately for the three regions of different types of elements and/or properties, that is: the ring, the grid beams and the distribution plate. These stresses were then compared with the limits of Appendix F and satisfied the required criteria.

CONCLUSION

An example of the application of substructuring in a dynamic analysis of non-linear integration was presented in this work. The interaction between two internal structures of PWR nuclear reactors was analyzed in the event of a LOCA. A F. E. model,

containing a super-element, was used to evaluate the forces and stresses caused by the impacts of the fuel elements on the grid.

The results obtained from the analysis of the second model, showed that: for primary stresses, the maximum loading caused by a cold leg LOCA on the lower grid is produced by the peak of the transient pressure gradient acting on the grid. This occurs when the fuel elements are separated from the grid. The impact of the fuel elements may produce high stresses in local regions of the grid, but these stresses are not important in LOCA. For the instants of maximum displacements of the super-element, the solution was expanded, obtaining in this way the stresses in the grid. These stresses satisfy the required criteria of the ASME Code.

REFERENCES

1 - Krieg, R. et al..1977. *Design of the HDR Experimental Program on Blowdown Loading and Dynamic Response of PWR Vessel Internals*. Nuclear Engineering and Design, 43, pp 419-435.

2 - Krieg, R.. 1982. *Review of LOCA Related Mechanical Problems and Analysis Methods*. Pressure Vessel and Piping: Design Technology - A Decade of Progress. ASME, pp 323-332.

3 - Marshall, W.. 1982. *An Assessment of the Integrity of PWR Pressure Vessels, Second Report*, UKAEA.

4 - Cloud, R. L.. 1978. *Structural Mechanics Applied to Pressurized Water Systems*. Nuclear Engineering and Design, 46, pp 273-302.

5 - ASME Boiler and Pressure Vessel Code, Section III, Division 1, Subsection NB and Appendices, 1989.

6 - Belytschko, T. and Liu, W.K.. 1985. *Computer Methods for Transient Fluid-Structure Analysis of Nuclear Reactors*. Nuclear Safety, 26(1), pp 14-31.

7 - Belytschko, T. and Schlechtendahl, E.G.. 1982. *Preface to the Special Issue: Fluid Structure Interaction and Internal Loading in Thermal Reactors*. Nuclear Engineering and Design, 70, pp 267-268.

8 - ANSYS User's Manual, revision 4.4. Swanson Analysis Inc., May/89.

9 - COPESP internal reports.